Laser Physics Letters

LETTER

High-energy azimuthally polarized laser beam generation from an actively Q-switched Nd:YAG laser with c-cut YVO_4 crystal

IOP Publishing | Astro Ltd

Laser Physics Letters

Laser Phys. Lett. 15 (2018) 055801 (5pp)

https://doi.org/10.1088/1612-202X/aaa6b3

Letter

High-energy azimuthally polarized laser beam generation from an actively *Q*-switched Nd:YAG laser with c-cut YVO_4 crystal

Jing Guo[1], Baofu Zhang[2], Zhongxing Jiao[2], Guangyuan He[1] and Biao Wang[1,2]

[1] Sino-French Institute of Nuclear Engineering and Technology, Sun Yat-sen University, Zhuhai 519082, People's Republic of China

[2] School of Physics, Sun Yat-sen University, Guangzhou 510275, People's Republic of China

E-mail: jiaozhx@mail.sysu.edu.cn and wangbiao@mail.sysu.edu.cn

Accepted for publication 10 January 2018
Published 14 March 2018

Abstract

A high-energy, azimuthally polarized (AP) and actively *Q*-switched Nd:YAG laser is demonstrated. The thermal bipolar lensing effect in the Nd:YAG laser rod is used as a polarization discriminator, and a *c*-cut YVO_4 crystal is inserted into the laser cavity to increase the mode-selecting ability of the cavity for AP mode. The laser generated AP pulses with maximum pulse energy as high as 4.2 mJ. To the best of our knowledge, this is the highest pulse energy obtained from an actively *Q*-switched AP laser. The pulse energy remained higher than 1 mJ over a wide range of repetition rates from 5 kHz to 25 kHz.

Keywords: azimuthally polarized laser beam, Nd:YAG laser, *c*-cut YVO_4 crystal

(Some figures may appear in colour only in the online journal)

Introduction

Radially polarized (RP) and azimuthally polarized (AP) beams have drawn much attention due to their unique properties [1], which can be used in many laser applications, such as optical manipulation [2], material processing [3–5] and vacuum laser acceleration [6]. Several methods are proposed to generate continuous wave (CW) RP and AP beams, including coherent superposition [7], linearly polarized beam transforming [8], intra-cavity mode selection with a conical Brewster prism [9], and photonic crystal mirrors [10]. In practice, there is a simple and effective method to produce RP and AP beams in solid-state lasers by using the thermal bipolar lensing effect in uniformly pumped isotropic solid-state rods [11]. Based on the fact that RP and AP beams focus differently in the laser rod, RP or AP beams can be easily obtained by using a specially designed cavity operating near the edge of the stable region. Another effective approach is to insert a *c*-cut crystal into the cavity to separate the RP and AP modes by using the large birefringence of the *c*-cut crystal; RP or AP beams can be obtained by simply adjusting the length of the cavity [12, 13].

Recently, RP and AP laser pulses were achieved via mode-locking or *Q*-switching [14–22]. By utilizing fiber Bragg gratings as the mode-selecting elements, all-fiberized lasers emitting RP and AP pulses were demonstrated with active mode-locking by a Mach–Zehnder intensity modulator [15], and passive mode-locking by a nonlinear amplifying loop mirror [16]. The minimum pulse duration was ~2 ns and the peak power was several hundred milliwatts in those all-fiber configurations. Nd:YAG-based RP and AP lasers mode-locked by acousto-optic modulators [17], semiconductor saturable absorber mirrors [18] and graphene [19] were

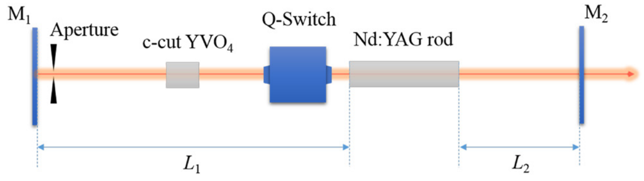

Figure 1. Experimental setup.

also demonstrated, with their pulse duration less than 150 ps and average power higher than 2 W at a repetition rate of 45–120 MHz. Compared to mode-locked lasers, Q-switched RP and AP lasers are more suitable for generating high-average-power beams with high pulse energy at kHz repetition rate. RP and AP beams passively Q-switched with Cr^{4+}:YAG crystal were demonstrated in Yb-doped fiber lasers [20, 21], a c-cut Nd:$GdVO_4$ laser [22] and Nd:YAG lasers [23, 24]. The maximum pulse energy was 0.12 mJ, as described in reference [24]. Through active Q-switching by an acousto-optic modulator, RP and AP beams were produced in a Nd:YAG laser with a photonic crystal grating as the mode selector. The pulse energy was 0.2 mJ at a repetition rate of 500 Hz [25]. Higher pulse energy was produced based on thermally induced birefringence in an actively Q-switched Nd:YAG laser; the maximum pulse energy reached 3 mJ at a repetition rate of 1.56 kHz [3].

In this paper, we present a high-energy actively Q-switched AP Nd:YAG laser based on the thermal bipolar lensing effect in the laser rod. A c-cut YVO_4 crystal is inserted into the laser cavity to increase the mode-selecting ability of the cavity for AP mode. A high-average-power AP laser with maximum pulse energy up to 4.2 mJ is obtained. The laser maintains stable operation over a wide range of repetition rates from 5 kHz to 25 kHz with pulse energy higher than 1 mJ.

Experiment design

The experimental setup is shown in figure 1; the laser cavity consisted of two flat mirrors, M_1 and M_2, an acousto-optical Q-switch, a Nd:YAG module, a c-cut YVO_4 crystal, and a mode-selecting aperture. M_1 and M_2 formed a plano–plano resonator, and M_2 also acted as an output coupler with transmission of 30% at lasing wavelength. The distance between M_1 and the left surface of the laser rod is labelled L_1, and the distance between right surface of the rod and M_2 (output coupler) is labelled L_2. The Nd:YAG rod was [1 1 1]-oriented and its doping concentration was 0.9 at.%, with a size of 4 mm in diameter and 120 mm in length. It was packaged in a five-laser-diode side-pumped module (Northrop Grumman, RD40-1C2 module) with a maximum pump power of 500 W. The c-cut YVO_4 crystal (CASIX Inc.) was 15 mm in length and 6 mm × 6 mm in aperture.

The key to achieving AP laser beams here is mode selecting through the aperture and bifocal effect of the Nd:YAG rod induced by the thermal bipolar lensing effect in the uniformly pumped isotropic solid-state rod. Due to the bifocal effect of the laser rod, the RP and AP beams have different mode-radii,

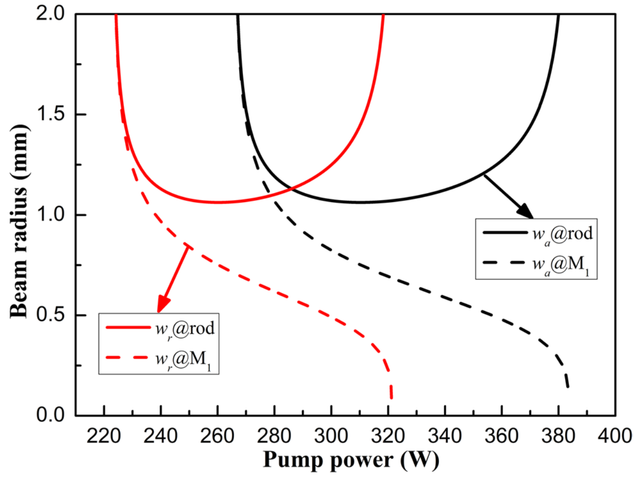

Figure 2. Stability zones of the resonator (w_a: the mode radius of the AP beam; w_r: the mode radius of the RP beam).

and they can be separated by inserting the aperture at the right position in the cavity. The AP beam is generated at the edge of the stability zones with high pump power, where the mode-radius of the RP beam becomes infinite and can be suppressed by the aperture. In order to obtain high-power AP beams, the stability zones of the AP mode operated under high pump power. According to the measured thermal lens of the Nd:YAG rod under different pump power, we obtained an optimum resonator with $L_1 = 800$ mm and $L_2 = 350$ mm, which gave the highest power with best beam quality. The stability diagrams for fundamental RP and AP beams (beam quality factor $M^2 = 2$) are shown in figure 2.

As shown in figure 2, the mode-radius of RP beam at the principle plane of the laser rod will become larger than the aperture of the laser rod when the pump power is over 320 W; the RP modes will be restrained, so only a high-power AP laser will be obtained. Under this case, the mode radius of the AP beam is smaller than the radius of the laser rod, thus high-order transverse modes may be generated. The aperture inserted near M_1 is to suppress the higher-order AP modes. However, too small an aperture will weaken the mode-selecting ability for AP beams because the radius of AP mode is larger than that of the RP mode at M_1, which is shown as dashed lines in figure 2. Therefore, an aperture with 2 mm in diameter was chosen in our experiment. An acousto-optical Q-switch (Gooch & Housego, QS27-6.5D-B) was inserted into the laser cavity to produce Q-switching operation and pulse output. When the laser is in Q-switched operation, the rod suffers from a process with thermal load changing periodically. It makes the thermal lensing become unstable and disturbs the AP mode operation. To obtain pure Q-switching AP beams, a c-cut YVO_4 crystal was inserted into the resonator, located 500 mm away from M_1. Due to the birefringence of the c-cut YVO_4 crystal, the RP and AP modes had different optical path lengths in the crystal, and hence the distribution of RP and AP beams in the cavity was changed [12]. This method further increased the separation of stability zones between RP and AP beams, which increased the mode-selecting ability of the cavity, and stable AP pulses were achieved.

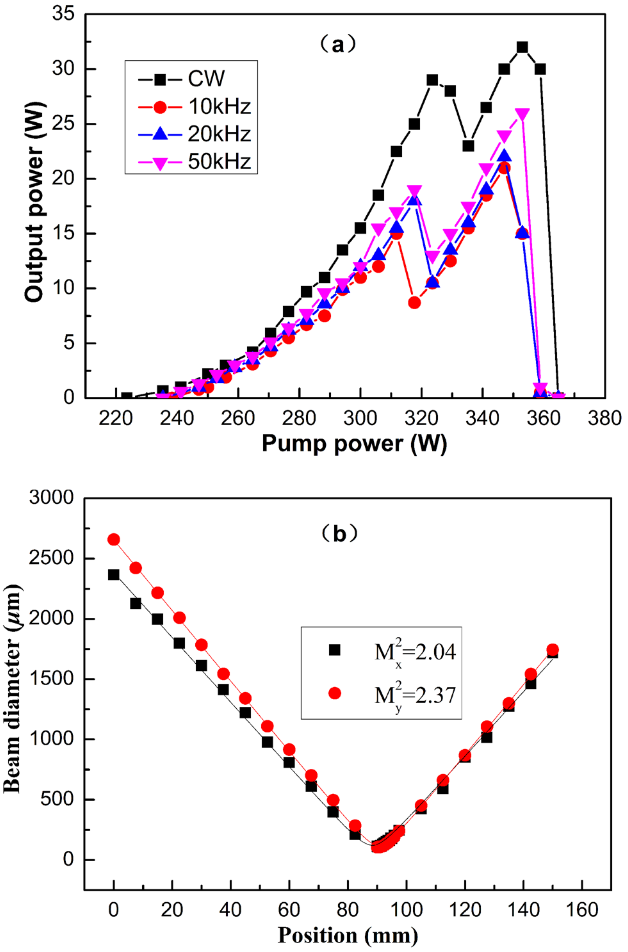

Figure 3. (a) Output power as a function of the pump power. (b) Beam quality of the CW AP beam.

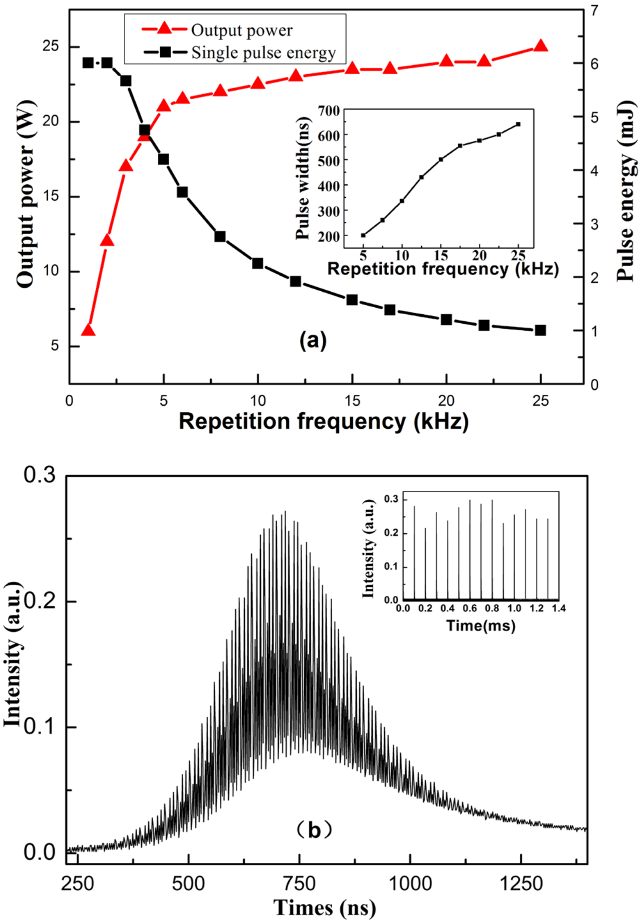

Figure 4. (a) Output properties at different repetition frequency (inset shows the pulse width at different repetition frequency). (b) Pulse shape at $f_r = 10$ kHz (inset is the pulse train).

Experiment results and discussions

Figure 3(a) shows the output power (measured by a Coherent Inc., PM300F-19) as a function of the pump power at different repetition frequency. In CW operation, the threshold was 230 W. When pump power reached 323 W, the output power began to decrease because the laser was getting out of the stability zone of the RP modes. The output power decreased to a local minimum average power of 23 W at the pump power of 335 W when RP modes were totally suppressed. When the pump power increased from 335 W to 360 W, AP laser beams with a doughnut-shaped cross section were obtained with a maximum average power of 32 W. These phenomena were consistent with the stability diagram shown in figure 2. The situation of Q-switching operation was similar to that of the CW operation. AP modes were also obtained at the local minimum point of the curve. The pump power of the minimum points became smaller at lower repetition frequency. The thermal lensing effect intensified due to the heavier thermal load of the rod at low repetition frequency, leading to stability zones moving towards the low pump power direction. The beam quality of the CW AP beam at pump power of 360 W was measured by a beam profiler (Thorlabs Inc., BP209); data are shown in figure 3(b). The M^2 factors were 2.04 and 2.37 in x- and y-directions, respectively. Both of them were close to the theory value of a fundamental AP beam (TE_{01} mode) of $M^2 = 2.0$.

Figure 4(a) shows the output power and pulse energy versus the repetition frequency (f_r) at the pump power of 350 W. When $f_r > 5$ kHz, the output power tends to saturate at about 25 W, and the beams appear as AP modes with a doughnut-shaped pattern. However, the output pulses become unstable when $f_r > 25$ kHz, and the output power decreases rapidly when $f_r < 5$ kHz. At low repetition rate $f_r = 3$ kHz, the thermal load-induced periodic fluctuations of the laser rod became obviously larger, and the polarization of the transverse mode became random. Thus, the proper repetition rate to generate stable AP beams here was between 5 kHz and 25 kHz. The pulse energy curve in figure 4(a) shows that the pulse energy decreases with increasing the repetition frequency. The maximum pulse energy of the stable AP laser was 4.2 mJ at the repetition frequency of 5 kHz. Even at a high repetition frequency of 25 kHz, the pulse energy of the AP beam was still larger than 1 mJ. The high pulse energy obtained here mainly benefited from the large volume of gain medium (4 mm in diameter), large beam mode-radius (larger than 1 mm as shown in figure 2), and the high working pump power (larger than 300 W) owing to our optimum resonator design.

The pulse width at different repetition frequencies was measured by using a fast detector (Thorlabs Inc., DET08CL),

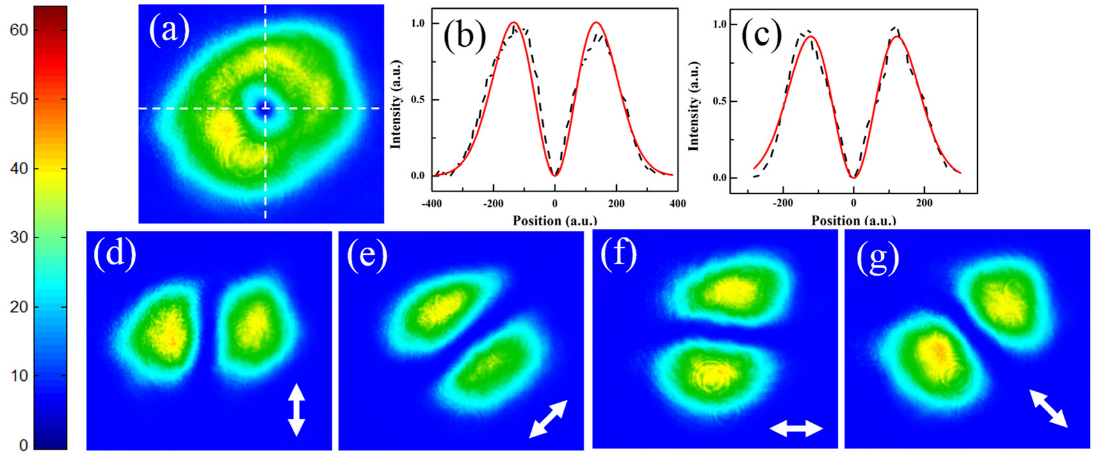

Figure 5. Beam profiles of far field. (a) Full beam profile. (b) and (c) Intensity distributions in horizontal and vertical axis. (d)–(g) Beam profiles after a linear polarizer; the arrows indicate the direction of polarizers.

and it is shown in the inset of figure 4(a). The pulse width increased with increasing the repetition frequency. The relatively large pulse width (several hundred nanoseconds) was due to the overall low net gain and long cavity round-trip time in the resonator. Figure 4(b) shows a typical pulse shape at $f_r = 10\,\mathrm{kHz}$ with the pulse train shown in the inset. The pulse duration is 336 ns, and multiple spikes emerged in the amplitude. The modulation depth of the pulse is over 50%. The time interval between the sub pulses is 8–12 ns, which agrees well with the intermode beat frequency (104.9 MHz) of the resonator.

The far-field beam profiles at different pump power and repetition rates were captured by a CCD (COHU Inc., 4812-7000/0000). Figure 5 shows a typical profile of the beam at pump power of 335 W and repetition frequency of 10 kHz. The beam profile had a doughnut shape; the intensity distributions in horizon and vertical axes are shown in figures 5(b) and (c), respectively. The experimental data is denoted by dashed lines, and the theory fitting of the profile of TE_{01} mode is denoted by solid lines. As shown in these two figures, the experimental results are in good agreement with the theoretical ones. Figures 5(d)–(g) show the beam profiles after a linear polarizer; the arrows indicate the direction of the polarizer. The two-lobe patterns are perpendicular to the directions of the polarizer. The polarization purity of the AP beam can be defined as the ratio between the intensity of azimuthally polarization and that of full beam at several positions of the cross section according to the data of the beam profiles [26]. The degrees of purity of the AP beam shown in figure 5 are ~86%, which indicates that the beam was a TE_{01} mode exactly.

The polarization purity of the AP beams at repetition frequency of 10 kHz under different pump power were calculated from the measured data and shown in figure 6. The pump power range from 323 W to 347 W corresponds to the AP operation region as shown in figure 3(a) (red line). When the pump power increased, the AP output increased from 10.5 W to 21 W, but the polarization purity degenerated from 94% to 80%, as shown in figure 6. Comparing to the stability diagram in figure 2, we can see that the highest pure AP beam was achieved at the outside edge of the RP stable region with a pump power of 323 W. This phenomenon was possibly caused by the aberrations of the thermal lens of the laser rod. In the ideal case of a perfectly uniform pumped laser rod, the thermal lens is spherical. However, the thermal lens is actually aspheric because of strong pump power in the center of the rod and non-radially symmetry of the arrangement of the pump sources. When increasing the pump power, the mode-radius of AP beam, which suffers serious influences from the aberrations of the thermal lens, enlarges as shown in figure 2 and deviates from paraxial. Thus, the polarization purity of AP beams degenerates, and the polarization purity of AP beams with smaller mode-radius is high at a relatively low pump power.

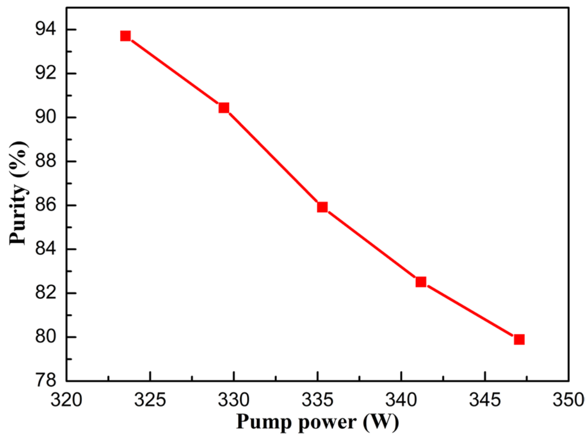

Figure 6. Polarization purity of AP beams at different pump power at 10 kHz repetition frequency.

Conclusion

In summary, we have demonstrated a high-energy actively Q-switched AP Nd:YAG laser. The thermal bipolar lensing effect in the Nd:YAG laser rod was used to separate the RP mode and AP mode. By using a c-cut YVO_4 crystal, the mode-selecting ability of the cavity for AP mode was increased.

Benefiting from the large volume of gain medium and the high pump power, we achieved high-pulse-energy AP radiation. At repetition rates from 5 kHz to 25 kHz, stable AP beams were obtained with pulse energy higher than 1 mJ. Moreover, an AP laser with maximum pulse energy up to 4.2 mJ and average power of 21 W was obtained at a repetition rate of 5 kHz. To the best of our knowledge, this is the highest pulse energy performance in an actively *Q*-switched AP laser.

Acknowledgements

This work was partially supported by the PhD Start-up Fund of Natural Science Foundation of Guangdong, China, under grant 2017A030310305, and Young Teachers Training Program of The Fundamental Research Funds for Sun Yat-sen University under grant 20174500031610017.

References

[1] Zhan Q 2009 Cylindrical vector beams: from mathematical concepts to applications *Adv. Opt. Photonics* **1** 1–57
[2] Kozawa Y and Sato S 2010 Optical trapping of micrometer-sized dielectric particles by cylindrical vector beams *Opt. Express* **18** 10828–33
[3] Meier M, Romano V and Feurer T 2007 Material processing with pulsed radially and azimuthally polarized laser radiation *Appl. Phys.* A **86** 329–34
[4] Gniziev V and Vnesterov A 1999 Influence of beam polarization on laser cutting efficiency *J. Phys. D: Appl. Phys.* **32** 1455–61
[5] Dorn R, Quabis S and Leuchs G 2003 Sharper focus for a radially polarized light beam *Phys. Rev. Lett.* **91** 233901–4
[6] Liu Y, Cline D and He P 1999 Vacuum laser acceleration using a radially polarized CO_2 laser beam *Nucl. Instrum. Methods Phys. Res.* A **424** 296–303
[7] Phua P B and Lai W J 2007 Simple coherent polarization manipulation scheme for generating high power radially polarized beam *Opt. Express* **15** 14251–6
[8] Machavariani G, Lumer Y, Moshe I, Meir A and Jackel S 2008 Spatially-variable retardation plate for efficient generation of radially- and azimuthally-polarized beams *Opt. Commun.* **281** 732–8
[9] Kozawa Y and Sato S 2005 Generation of a radially polarized laser beam by use of a conical Brewster prism *Opt. Lett.* **30** 3063–5
[10] Kozawa Y and Sato S 2010 Demonstration and selection of a single-transverse higher-order-mode beam with radial polarization *J. Opt. Soc. Am.* A **27** 399
[11] He G, Guo J, Wang B and Jiao Z 2011 Generation of radially polarized beams based on thermal analysis of a working cavity *Opt. Express* **19** 18302–9
[12] Yonezawa K, Kozawa Y and Sato S 2006 Generation of a radially polarized laser beam by use of the birefringence of a *c*-cut Nd:YVO_4 crystal *Opt. Lett.* **31** 2151–3
[13] Kozawa Y, Yonezawa K and Sato S 2007 Radially polarized laser beam from a Nd:YAG laser cavity with a *c*-cut YVO_4 crystal *Appl. Phys.* B **88** 43–6
[14] Mandujano M G and Maytorena J A 2013 Quadrupolar second-harmonic generation by helical beams and vectorial vortices with radial or azimuthal polarization *Phys. Rev.* A **88** 023811–6
[15] Zhou Y, Wang A, Gu C, Sun B, Xu L, Li F, Chung D and Zhan Q 2016 Actively mode-locked all fiber laser with cylindrical vector beam output *Opt. Lett.* **41** 548–50
[16] Sun B, Wang A, Gu C, Chen G, Xu L, Chung D and Zhan Q 2015 Mode-locked all-fiber laser producing radially polarized rectangular pulses *Opt Lett* **40** 1691–4
[17] Enderli F and Feurer T 2009 Radially polarized mode-locked Nd:YAG laser *Opt. Lett.* **34** 2030–2
[18] Huang J, Deng J, Cao Y, Weng W, Zheng H, Li J, Shi F, Ge Y, Dai S and Lin W 2011 Passively mode-locked radially polarized laser based on ceramic Nd:YAG rod *Opt. Express* **19** 2120–5
[19] Li L, Ren Z, Chen X, Qi M, Zheng X, Bai J and Sun Z 2013 Passively mode-locked radially polarized Nd-doped yttrium aluminum garnet laser based on graphene-based saturable absorber *Appl. Phys. Express* **6** 082701
[20] Lin D, Xia K, Li R, Li X, Li G, Ueda K and Li J 2010 Radially polarized and passively *Q*-switched fiber laser *Opt. Lett.* **35** 3574–6
[21] Zou L, Yao Y, Han X H, Liu J Y, Xu Y and Li J L 2015 Azimuthally polarized, passively *Q*-switched Yb-doped fiber laser *Opt. Commun.* **355** 181–5
[22] Chang K C, Li D L and Wei M D 2014 Self-sustaining azimuthal polarization in a passively *Q*-switched Nd:$GdVO_4$ laser with a Cr^{4+}:YAG saturable absorber *J. Opt. Soc. Am.* B **31** 382–6
[23] Li J, Ueda K, Musha M, Zhong L and Shirakawa A 2008 Radially polarized and pulsed output from passively *Q*-switched Nd:YAG ceramic microchip laser *Opt. Lett.* **33** 2686–8
[24] Fang Z Q, Xia K G, Yao Y and Li J L 2015 Radially polarized and passively *Q*-switched Nd:YAG laser under annular-shaped pumping *IEEE J. Sel. Top. Quantum Electron.* **21** 1–6
[25] Xia K G, Ueda K I and Li J L 2012 Radially polarized, actively *Q*-switched, and end-pumped Nd:YAG laser *Appl. Phys.* B **107** 47–51
[26] Machavariani G, Lumer Y, Moshe I, Meir A, Jackel S and Davidson N 2007 Birefringence-induced bifocusing for selection of radially or azimuthally polarized laser modes *Appl. Opt.* **46** 3304–10